Evaluation of Stability Margin of Active Magnetic Bearing Control System Combined with Several Filters

Makoto Ito

Dept. of Mechanical Engineering, National Defense Academy
1-10-20 Hashirimizu, Yokosuka-shi, Kanagawa, 239-8686, Japan
g41063@nda.ac.jp

Hiroyuki Fujiwara

Dept. of Mechanical Engineering, National Defense Academy
hiroyuki@nda.ac.jp

Naohiko Takahashi

Hitachi Industries Co. Ltd., Tsuchiura, Ibaraki, 300-0013, Japan
naohiko_takahashi@pis.hitachi.co.jp

Osami Matsushita

Dept. of Mechanical Engineering, National Defense Academy
osami@nda.ac.jp

ABSTRACT

Flexible rotors supported by Active Magnetic Bearings(AMBs) have problems with high frequency instabilities called spillover instability. ISO 14839 series provides a standard about AMBs equipped rotors and Part 3 intends to regulate the stability and sensitivity of any eigen modes existing in the rotational speed and high frequency domain. The peaks of the sensitivity function become the index for judging stability margin.

In this paper, the stability margins of several controllers are evaluated by the sensitivity function. We used the PID controllers with several filters which is applied to avoid spillover instability and performed the experiment of levitation at 0rps. The field data about the stability evaluation by the sensitivity function is obtained.

INTRODUCTION

In order to design an Active Magnetic Bearing (AMB) control system, firstly, critical speeds appearing within the rated number of revolutions must be damped sufficiently. ISO 10814 specifies these criteria as a Q-factor for unbalance resonance. Since a rotor has many high-frequency eigen modes, it easily oscillates at bending mode frequencies higher than the rated one, which is called spill-over. Secondly, measures must be taken against this problem. Many kinds of control system design have been proposed to solve the spill-over problem [1, 2].

Regarding the stability of the AMB control system (free vibration system), ISO CD 14839-3 is going to define criteria for evaluating the stability margin based on the sensitivity function. Of all eigen modes appearing not only within the rated speed but also at higher frequencies, the mode having the highest sensitivity is evaluated according to the stability margin. In past studies, there have been few reports on the evaluation of the stability margin based on the sensitivity function of the AMB control system [3].

This paper describes how to design a variety of controllers used for AMB-supported symmetrical and flexible rotors according to the phase adjustment method, and reports results of the evaluation of stability margins given by the designed controllers through the sensitivity function. We believe that the measured data of the sensitivity functions resulting from this study suggests important guidelines (ISO standards) for designing the controllers.

2. FLEXIBLE ROTOR

2.1 Flexible rotor's specifications

Figure 1 illustrates the structure of a flexible rotor. The length is 1,310 mm, the mass is 31.4 kg, and the shaft diameter is 37 mm. The rotor includes radial AMBs inserted onto both sides, a thrust disk attached to the left end, and a non-contact flat motor disk fixed to the right end.

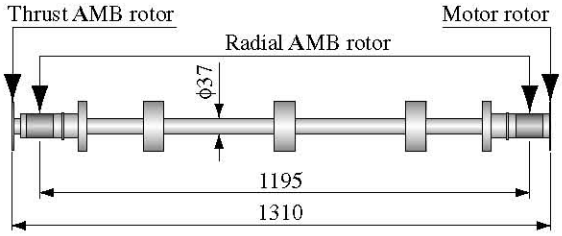

FIGURE 1: Structure of flexible rotor

2.2 Vibration modes of the flexible rotor

In this study, we used the mode synthesis method [4,5] to create a 7 DOF model and analyzed up to the fifth

bending mode Nc7, expected to be the spill-over point.

Figure 2 shows the vibration modes of the rotor when a free-free condition is given. Since the AMBs are supported flexibly, the rotor should have vibration modes as indicated in Figure 2 at each critical speed. Nc1 and Nc2 are the rigid mode's critical speeds, and Nc3,Nc4 (Nc5, Nc6,Nc7 are omitted) are the bending mode's critical speeds.

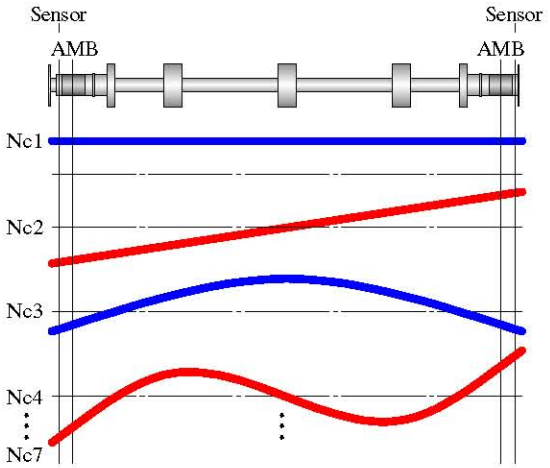

FIGURE 2: Modes of the flexible rotor

3. CONTROLLER

3.1 Controller configuration

Figure 3 is the block diagram of a digital controller. We control the rotor using the mode separation method [6,7]. Signals fed from the displacement sensors arranged near to the right and left radial AMBs are divided into translating and tilting modes by the simple equation shown in the figure. Each of the separated signals is reformed by the different controllers and fed to the power amplifier (PWM). Note that the translating modes Nc1, Nc3, ... (odd numbers) show that the rotor displacements are in-phase with each other at both ends where the radial AMBs are arranged, while the tilting modes Nc2, Nc4, ... (even numbers) indicate that those are in opposite phase.

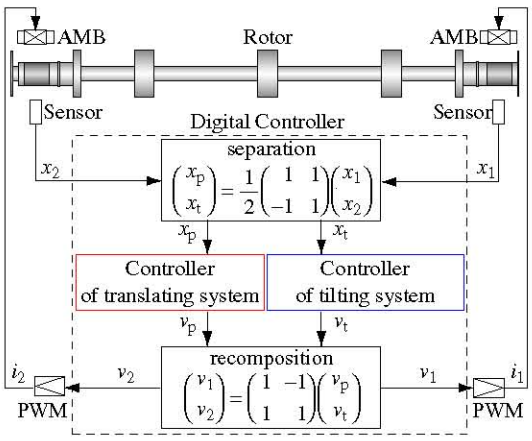

FIGURE 3: Block diagram of a digital controller

3.2 Plant transfer functions after the mode separation

Figure 4(a) shows the measured plant transfer function $|G_{pp}|$ of the translating system after mode separation, while Figure 4(b) presents the measured plant transfer function $|G_{pt}|$ of the tilting system. The translating system (rigid mode, Nc3, Nc5, Nc7, ...) and the tilting system (rigid mode, Nc4, Nc6, ...) are successfully separated from each other. We designed controllers for each system separated.

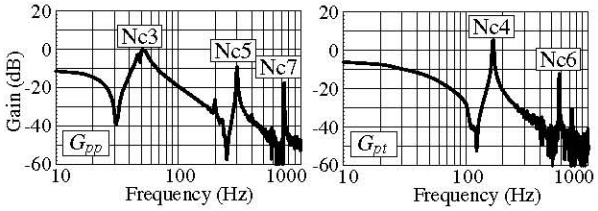

(a) Translating system (b) Tilting system

FIGURE 4: Bode plot of the system

3.3 Designing translating controllers

We incorporated various filters into translating controllers to adjust the phase. The three controllers we designed are shown below:

= Controller **p1**:

$$G_{rp1} = G_{PID1} \times G_{NF1} \tag{1}$$

= Controller **p2**:

$$G_{rp2} = G_{PID1} \times G_{NF1} \tag{2}$$

= Controller **p3**:

$$G_{rp3} = G_{PID2} \times G_{PSF1} \tag{3}$$

where,

$$G_{PID1} = 0.5(G_I + G_{PL1} + G_{PL2})$$

$$= 0.5\left(\frac{240}{\tau_1 s+1} + \frac{\tau_2 s+1}{\alpha_1\tau_2 s+1} + \frac{\tau_3 s+1}{\alpha_2\tau_3 s+1}\right)$$

$$G_{PID2} = 0.5(G_I + G_{PL2} + G_{PL3})$$

$$= 0.5\left(\frac{240}{\tau_1 s+1} + \frac{\tau_3 s+1}{\alpha_2\tau_3 s+1} + \frac{\tau_4 s+1}{\alpha_3\tau_4 s+1}\right)$$

$$G_{PBF} = \frac{1}{1-\alpha_1}\left(1 - \frac{\alpha_1}{(\tau_5 s)^2 + 2\zeta_1(\tau_5 s)+1}\right)$$

$$G_{NF1} = \frac{(\tau_6 s)^2 + 1}{(\tau_6 s)^2 + 2\zeta_2(\tau_6 s)+1}$$

$$G_{PSF1} = \frac{(\tau_5 s)^2 - 2\zeta_2(\tau_5 s)+1}{(\tau_7 s)^2 + 2\zeta_3(\tau_7 s)+1}$$

G_{PID} is a PID control circuit, G_I is an Integrator, G_{PL} is a Phase Lead Circuit, G_{PBF} is a Phase Bump Filter (PBF), G_{NF} is a Notch Filter (NF), and G_{PSF} is a Phase Shifting Filter (PSF). The other parameters are shown below:

$\tau_1 = 1/(2\pi 0.1)$, $\tau_2 = 1/(2\pi 10)$, $\tau_3 = 1/(2\pi 100)$, $\tau_5 = 1/(2\pi 1000)$, $\tau_6 = 1/(2\pi 710)$, $\tau_4 = 1/(2\pi 50)$, $\tau_7 = 1/(2\pi 650)$, $\alpha_1 = 0.4$, $\alpha_2 = 0.1$, $\alpha_3 = 0.3$, $\zeta_1 = 0.46$, $\zeta_2 = 0.05$, and $\zeta_3 = 0.06$

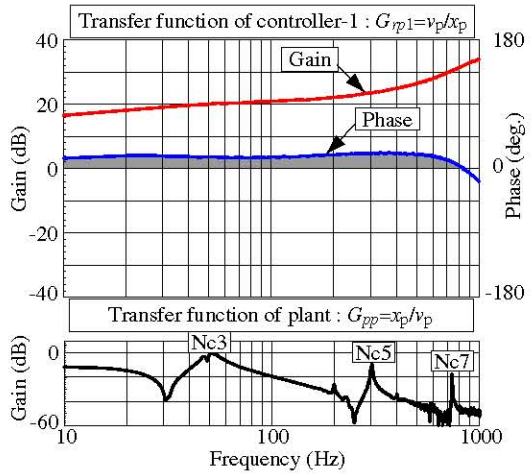

FIGURE 5: Bode plot of Controller **p1**

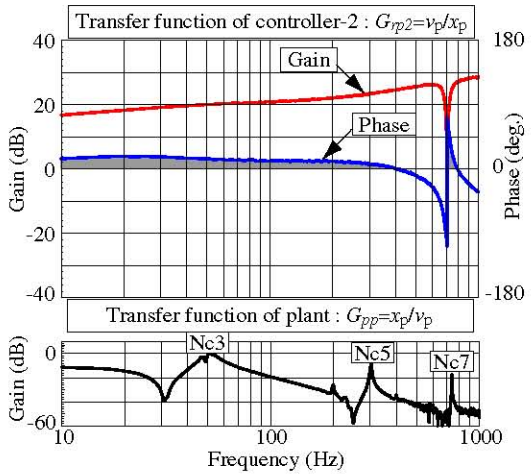

FIGURE 6: Bode plot of Controller **p2**

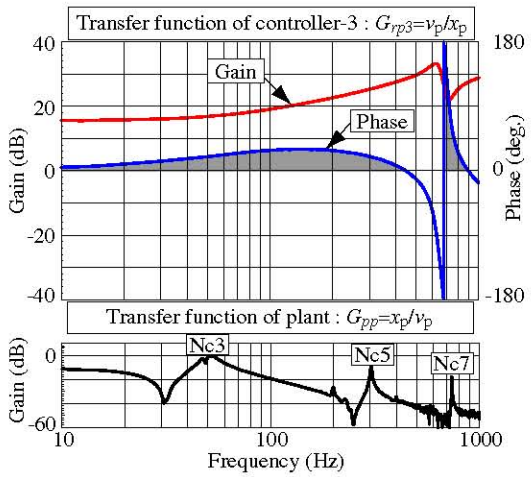

FIGURE 7: Bode plot of Controller **p3**

Figures 5, 6, and 7 show the measured Bode plots of controllers **p1**, **p2**, and **p3,** respectively, with the measured plant transfer functions $|G_{pp}|$ of the translating system. The translating controllers are designed to advance the phases of the eigen modes of the translating system indicated in Figure 4(a) so as to ensure positive damping.

- Controller **p1**:
  Nc1-Nc7: Damped by Phase Lead Circuit + PBF.
- Controller **p2**:
  Nc1, Nc3, and Nc5: Damped by Phase Lead Circuit.
  Nc7: Addressed by NF (measure for spill-over).
- Controller **p3**:
  Nc1, Nc3, and Nc5: Damped by Phase Lead Circuit.
  Nc7: Addressed by PSF (measure for spill-over).

3.4 Designing tilting controllers

In the same fashion as the translating controllers, we designed the following three tilting controllers:

- Controller **t1**:

$$G_{rt1} = G_{rp1} = G_{PID1} \times G_{PBF1} \tag{4}$$

- Controller **t2**:

$$G_{rt2} = G_{PID3} \times G_{NF2} \tag{5}$$

- Controller **t3**:

$$G_{rt3} = G_{PID4} \times G_{PSF2} \times G_{2LPF} \tag{6}$$

where,

$$G_{PID3} = 0.5(G_I + G_{PL1} + G_{PL4}) = 0.5\left(\frac{240}{\tau_1 s+1} + \frac{\tau_2 s+1}{\alpha_1\tau_2 s+1} + \frac{\tau_8 s+1}{\alpha_4\tau_8 s+1}\right)$$

$$G_{PID4} = 0.5(G_I + G_{PL5}) = 0.5\left(\frac{240}{\tau_1 s+1} + \frac{\tau_9 s+1}{\alpha_3\tau_9 s+1}\right)$$

$$G_{NF2} = \frac{(\tau_{10}s)^2+1}{(\tau_{10}s)^2 + 2\zeta_2(\tau_{10}s)+1}$$

$$G_{PSF2} = \frac{(\tau_{12}s)^2 - 2\zeta_5(\tau_{12}s)+1}{(\tau_{11}s)^2 + 2\zeta_4(\tau_{11}s)+1}$$

$$G_{2LPF} = \frac{1}{(\tau_{13}s)^2 + 2\zeta_6(\tau_{13}s)+1}$$

G_{2LPF} is a second-order low-pass filter (2nd LPF), and the other parameters are shown below:

$\tau_8 = 1/(2\pi 80)$, $\tau_9 = 1/(2\pi 35)$, $\tau_{10} = 1/(2\pi 550)$, $\tau_{11} = 1/(2\pi 113)$, $\tau_{12} = 1/(2\pi 153)$, $\tau_{13} = 1/(2\pi 300)$, $\alpha_4 = 0.13$, $\zeta_4 = 0.109$, $\zeta_5 = 0.084$, and $\zeta_6 = 0.12$

Figures 8, 9, and 10 show the measured Bode plots of controllers **t1**, **t2**, and **t3,** respectively, with the plant transfer functions $|G_{pt}|$ of the tilting system. The tilting controllers are designed to advance the phases of the eigen modes of the tilting system shown in Figure 4(b) in order to ensure positive damping. Note that the same controller is used for **t1** and **p1**.

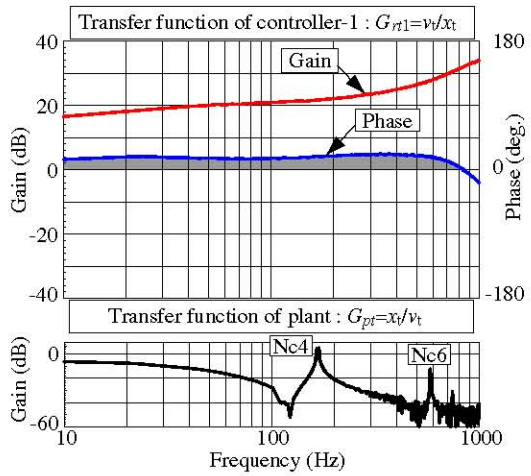

FIGURE 8: Bode plot of Controller **t1**

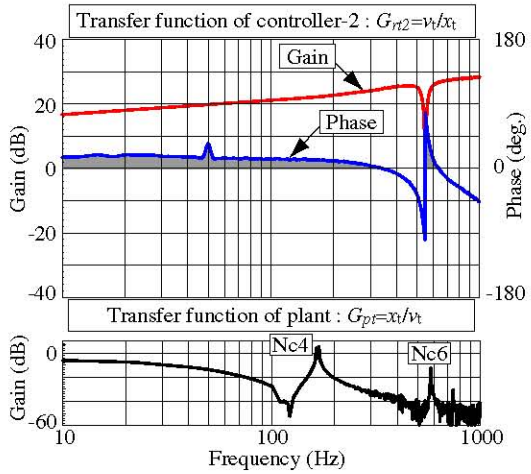

FIGURE 9: Bode plot of Controller **t2**

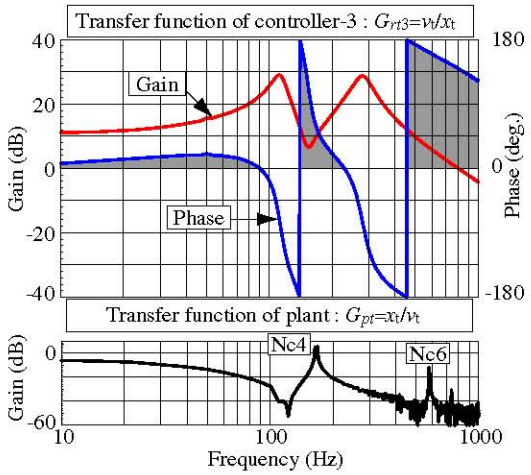

FIGURE 10: Bode plot of Controller **t3**

= Controller **t1**:
Nc2-Nc6: Damped by Phase Lead Circuit + PBF.

= Controller **t2**:
Nc2 and Nc4: Damped by Phase Lead Circuit.
Nc6: Addressed by NF (countermeasure for spill-over).

= Controller **t3**:
Nc2: Damped by Phase Lead Circuit.
Nc4: Addressed by PSF (countermeasure for spill-over).
Nc6: Addressed by 2nd-order LPF (same as above).

4. EVALUATING THE STABILITY MARGIN

4.1 Control system configuration

With the sensitivity function, ISO CD 14839-3 defines criteria for evaluating the stability margin of the AMB-supported flexible rotor used in this study. The sensitivity function is represented by the following equation:

$$G_S = \frac{1}{1+G_O} \tag{7}$$

where G_O is the open-loop transfer function.

Table 1 lists allowable stability margins (sensitivities) defined by ISO. In Zone A, the best condition, the sensitivity must be 8 dB or less. Table 2 lists control systems consisting of various combinations of the translating and tilting controllers designed in this study. We evaluated the stability margins on a system basis.

TABLE 1: Peak sensitivity at zone limits

Zone	Peak sensitivity	
	level	factor
A/B	8 dB	2.5
B/C	12 dB	4
C/D	14 dB	5

TABLE 2: AMB control system

System No.	Controller	
	Translating controller	Tilting controller
1	Controller **p1**	Controller **t1**
2	Controller **p2**	Controller **t2**
3	Controller **p3**	Controller **t3**
4	Controller **p2**	Controller **t3**
5	Controller **p3**	Controller **t2**

4.2 Evaluating the stability margin based on the sensitivity function

We simulated System 1 and describe how to evaluate it through the sensitivity function.

Figure 11 shows the dB Nyquist plots of System 1 derived from the open-loop transfer functions of the translating and tilting systems. In the dB Nyquist plot the gain axis is represented in dB (logarithm scale), and the = mark indicates 0 dB that corresponds to the critical point (-1,0) of normal Nyquist plots. Accordingly, these figures show that the translating and tilting systems of System 1 are stable.

As represented by equation (7), the sensitivity function is the reciprocal of a distance from the critical point (0 dB) to the trajectory G_O in the Nyquist plots of Figure 11. Therefore, the shorter the distance, the higher the sensitivity G_S; conversely, the longer the distance, the lower the sensitivity. This means that the sensitivity function can evaluate the system stability margin.

In this study, we evaluated all the modes except Nc1 and Nc2, the rigid modes of the translating and tilting systems respectively. This is because it is easy to change the nature of the phase lead circuit applied to the rigid modes, which allows the adjustment of the phase lead (damping ratio ζ) so that sensitivities are within Zone B.

Figure 12 indicates the sensitivity functions of the translating and tilting systems of System 1. It shows that Nc7 has a sensitivity of 15 dB, the highest in the translating system. This value is in Zone D specified by ISO, which suggests that the rotor may be mechanically broken during operation. In the tilting system, Nc6 has a sensitivity of 10 dB, the highest except for the rigid mode Nc2, and is in Zone B of ISO, which suggests that the rotor can run for long hours. These results show that System 1 is hard to run unless the translating controller is modified.

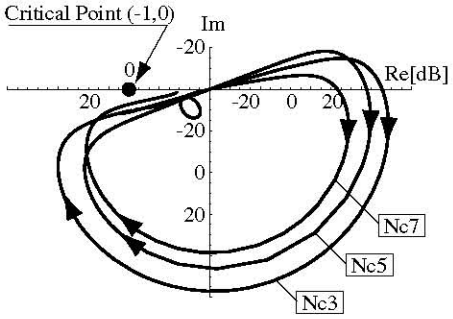

(a) Translating system

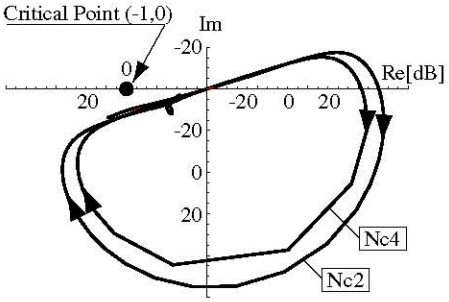

(b) Tilting system

FIGURE 11: Nyquist plots of System 1 (dB polar)

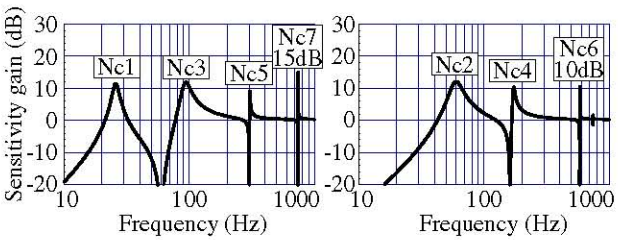

(a) Translating system (b) Tilting system

FIGURE 12: Sensitivity functions of System 1

4.3 Experimental evaluation of the stability margins

This subsection provides results from experiments for evaluating the stability margins of the various control systems listed in Table 2 when the rotor is levitated statically (at 0 rpm).

Figure 13 shows the measured sensitivity functions of the translating and tilting systems of System 1. Nc7 has a sensitivity of 17 dB (Zone D), the highest in the translating system, while Nc6 has a sensitivity of 10 dB (Zone B), the highest in the tilting system. These experimental results are close to the simulated ones given in Subsection 4.2. In System 1, adding the PBF to the controller increases the sensitivity of the high-frequency eigen mode appearing in a high-frequency band (having its center frequency at about 800 Hz) where the phase lead is smaller.

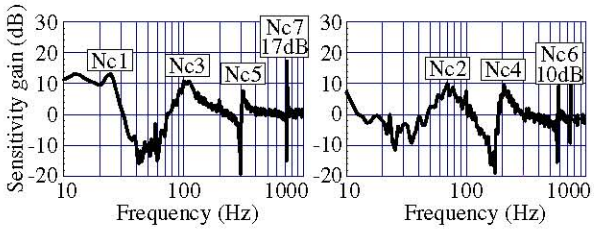

(a) Translating system (b) Tilting system

FIGURE 13: Sensitivity functions of System 1

Figure 14 shows the measured sensitivity functions of the translating and tilting systems of System 2. Nc5 has a sensitivity of 16 dB (Zone D), the highest in translating system, while Nc4 has a sensitivity of 14 dB (Zone C), the highest in the tilting system. In System 2, adding the NF to the controller reduces the phase advance of the eigen mode right before that to which the filter is applied, which increases the sensitivities of Nc5 and Nc4 appearing in the translating and tilting systems, respectively.

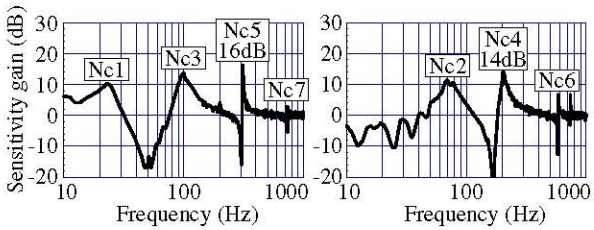

(a) Translating system (b) Tilting system

FIGURE 14: Sensitivity functions of System 2

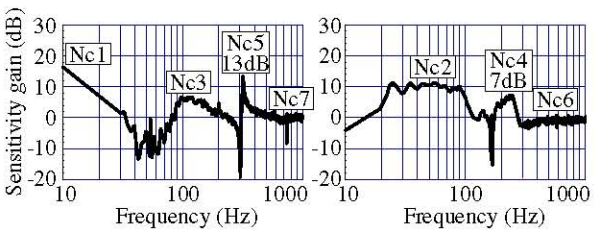

(a) Translating system (b) Tilting system

FIGURE 15: Sensitivity function of System 3

Figure 15 presents the measured sensitivity functions of the translating and tilting systems of System 3. In the translating system, Nc5 has a maximum sensitivity of 13 dB (Zone C), while in the tilting system, Nc4 has a maximum sensitivity of 7 dB (Zone A). In System 3, applying the PSF to the translating controller shows the same phenomenon as the NF, that is, the sensitivity of Nc5—the eigen mode right before the applied one is higher. However, it is lower than the sensitivity given by the NF, and also the sensitivity of the applied eigen mode Nc7 is very low. As shown in the tilting controller, the combination of the PSF and 2nd-order LPF can suppress the sensitivities of Nc4 and Nc6 to which the PSF and 2nd-order LPF is respectively applied.

Figure 16 shows the measured sensitivity functions of the translating and tilting systems of System 4. In the translating system, Nc5 has a maximum sensitivity of 17 dB (Zone D), while in the tilting system, Nc4 has a maximum sensitivity of 4 dB (Zone A). Since System 4 has the same translating controller as System 2, the experimental results are similar to those of System 2. Moreover, System 4 has the same tilting controller as System 3, which gives experimental results similar to those of System 3, except for the sensitivity of Nc4 which is a little lower.

Figure 17 presents the measured sensitivity functions of the translating and tilting systems of System 5. The translating system shows Nc5 has a maximum sensitivity of 10 dB (Zone B), while the tilting system indicates Nc4 has a maximum sensitivity of 12 dB (Zone B). Since System 5 has the same translating controller as System 3, the experimental results are close to those of System 3. Moreover, System 5 has the same tilting controller as System 2, which gives almost the same experimental results as those of System 2.

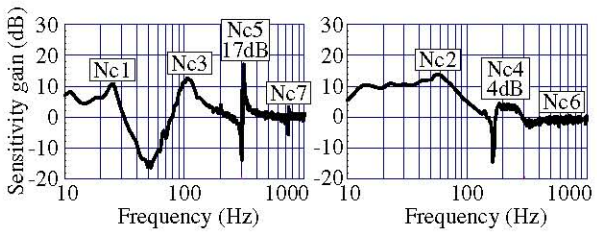

(a) Translating system (b) Tilting system

FIGURE 16: Sensitivity function of System 4

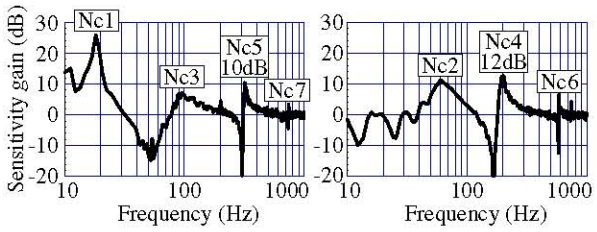

(a) Translating system (b) Tilting system

FIGURE 17: Sensitivity function of System 5

5. CONCLUSION

In this paper, we have designed various controllers for the AMB-supported symmetrical and flexible rotor to evaluate the stability margins of the system through the sensitivity functions. Table 3 summarizes the experimental results. Of the systems built in this study, System 5 has the largest stability margin to allow the rotor to run stably.

We believe that the data obtained by this study as elementary data, is valuable for the establishment of guidelines (ISO standards) for designing controllers used for the AMB.

We would like to thank the New Energy and Industrial Technology Development Organization (NEDO) for their invaluable help in conducting our study.

TABLE 3: Evaluation of the stability margins

System No.	Peak sensitivity level (dB)					Zone
	Nc3	Nc4	Nc5	Nc6	Nc7	
1	11		8		17	D
		10		10		B
2	14		16		3	D
		14		7		C
3	6		13		1	C
		7		1		A
4	12		17		3	D
		4		1		A
5	7		10		3	B
		12		6		B

REFERENCE

[1] Tagawa, Y., Yamada, G., Modeling and Control of a Flexible Structure System (Suppression of Spill-Over Instability), Trans. of JSME, Vol.54, No.505, pp.2111-2117, 1988 (in Japanese).

[2] Naohiko Takahashi, et. al., Control of Flexible Rotors Supported by Active Magnetic Bearing, Trans. of JSME, Vol.61, No.588, pp.3228-3233, 1995 (in Japanese).

[3] Hirohuki Fujiwara, et. al., Control of Flexible Rotors Supported by Active Magnetic Bearings, *Proc. Dynamics and Design Conference 2002*, CD-ROM No.724, 2002 (in Japanese).

[4] Osami Matsushita, et. al., Modeling: Free from Boundary Condition, Trans. of JSME, Vol.51, No.588, pp.44-48, 1988 (in Japanese).

[5] Makoto Ito, et. al., Unbalance vibration Control for High Order Bending Critical Speeds of Flexible Rotor Supported by Active Magnetic Bearing, *Proc. 8th Int. Symp. On Transport Phenomena and Dynamics of Rotating Machinery*, pp.923-928, 2000

[6] G. Schweizer, H. Bleuler, A. Traxler, Active Magnetic Bearings, Verlag der Fachvereine (vdf), ETH-zurich, 1994.

[7] Hirohuki Fujiwara, et. al., Control of Flexible Rotors Supported by Active Magnetic Bearings, *Proc. 8th Int. Symp. On Magnetic Bearing*, pp.145-150, 2002.